Int. J. Electrochem. Sci., 14 **(2019)** 7871 – 7883, doi: 10.20964/2019.08.48

International Journal of
ELECTROCHEMICAL
SCIENCE
www.electrochemsci.org

Electrochemical Performance of the Pd/C Catalyst Synthesized by Polyol Process

Shaofeng Yu[1], *Qiong Han*[1], *Yingjia Yang*[1], *Xuli Ma*[1], *Lizhen Gao*[1], *Shaohui Yan*[1,*], *Yucheng Wu*[2,*], *Liquan Lu*[3]

[1] College of Environmental Science and Engineering, Taiyuan University of Technology, Taiyuan, 030024, China
[2] MOE Key Laboratory for Interface Science and Engineering in Advanced Materials and Research Center of Advanced Materials Science and Technology, Taiyuan University of Technology, Taiyuan, 030024, China
[3] College of Mechatronic Engineering, North University of China, Taiyuan 030051, China
[*]E-mail: yanshaohui@tyut.edu.cn, wyc@tyut.edu.cn

Received: 2 April 2019/ *Accepted:* 24 May 2019 / *Published:* 30 June 2019

Apolyol process is employed to synthesize Pd nanoparticles supported on carbon (Pd/C), for developing an electrocatalyst with excellent performance for methanol oxidation. The results show that this method has a high efficiency for the Pd nanoparticles depositing on the carbon support. Moreover, the average diameter of the Pd nanoparticles decreases with the amount of KOH solution employed during the catalyst synthesis. The highest electrochemical activity of the Pd/C catalyst for the methanol oxidation in 0.1 M KOH solution with 1.0 M methanol at 25 ^{o}C reaches to 447.4 mA mg^{-1} Pd. The activity difference between the Pd/C catalysts prepared at 200 (447.4 mA mg^{-1} Pd) and 180 ^{o}C (435.8 mA mg^{-1} Pd) for the methanol electrooxidation is very small, showing that the polyol process is suitable for the preparation of the Pd/C.

Keywords: Direct methanol fuel cells (DMFCs), Pd nanoparticles, Methanol electrooxidation, Electrocatalysis, Nanomaterials

1. INTRODUCTION

Direct methanol fuel cells (DMFCs) have attracted worldwide attention due to their low temperature and fast start-up, clean fuel and environmental protection, and simple battery structure [1,2]. Methanol produces CO_3^{2-} and H_2O in an alkaline environment, which includes two reactions [3-5]:

$$CH_4O + H_2O \rightarrow CO_2 + 6H^+ + 6e^- \quad (1)$$

$$2OH^- + CO_2 \rightarrow CO_3^{2-} + H_2O \quad (2)$$

The success of methanol fuel cells depends to a large extent on the performance of the electrocatalyst. With regard to the new DMFCs anode catalyst, there are two main challenges, namely performance, including activity, reliability and durability, as well as cost reduction [1]. So far, the most advanced electrocatalyst is Pt metal. The mechanism of methanol oxidation on the surface of Pt has been extensively studied. The main process includes several steps, such as: (1) methanol adsorption; (2) C–H bond activation (methanol dissociation); (3) water adsorption; (4) water activation; (5) CO oxidation [1]. But the high cost of Pt is still a challenge for its widespread application [6]. Alternatively, Pd metal has a high degree of abundance in nature [6,7]. In addition, Pd-based catalysts have stronger CO tolerance and exhibit good catalyst activity in alkaline media, making it becomes a substitute for Pt [6,10].

The function of electrocatalysts strongly depends on surface area, number of active sites and conductivity [11,12]. Therefore, a lot of preparation methods have been tried to optimize these features. Improving the microstructure of the catalyst to optimize size, shape and surface morphology is a typical strategy to improve electrocatalytic activity [13-16]. Reducing agents and stabilizers are used in most methods. Commonly reducing agents, such as sodium borohydride and hydrazine, can seriously harm human health and the natural environment, which limits their practical use in catalyst preparation [17]. Stabilizers, such as polyvinylpyrrolidone (PVP) and oleylamine, prevent the aggregation of metal nanoparticles, but the stabilizer is strongly adsorbed on the surface of the metal nanoparticles, occupying many active sites, and reducing the activity of the catalyst significantly [18-21]. In addition, the preparation method has a crucial influence on the performance of the catalyst. The conventional impregnation method is difficult to control the particle size, the colloidal method is troublesome to operate and is not suitable for large-scale preparation of future electrocatalysts, and the electrodeposition method is difficult to achieve uniform deposition on a large-area upper electrode [22]. Therefore, it is necessary to introduce a simple method, which is free of stabilizers, for preparing Pd/C (activated carbon supported Pd nanoparticles).

In this work, a polyol process is employed to prepare a Pd/C catalyst. There is no stabilizer in this process, and ethylene glycol is used as both solvent and reducing agent in this method, since the reducing CH_3CHO species will be produced when ethylene glycol is heated in alkaline media [23-25]. The results show that the method exhibits excellent metal utilization rate, and Pd metal nanoparticles are uniformly dispersed on the carbon support on the prepared Pd/C catalyst, and exhibit excellent catalytic performance for methanol electrooxidation (MEO).

2. EXPERIMENTAL

2.1 Synthesis of Pd/C catalysts

The Pd/C catalyst is prepared by a polyol process. Firstly, 0.048 g vulcan XC-72R activated carbon is dispersed in 2 ml 0.0564 M $PdCl_2$ solution and 80 ml ethylene glycol using ultrasonic agitation for 30 min. After that, the proper amount of 1 M KOH aqueous solution is added into the suspension for adjusting its pH. The amount of KOH aqueous solution is selected to start from 3.4 ml,

adjusting the suspension to alkalescency. Then, it is poured in a Teflon-lined stainless steel autoclave, which is then put in an oven to be heated to 200 or 180 ºC for 6 h. After the reaction mixture is cooled down to ambient temperature, about 50 ml ethanol is added into it to dilute [23]. Where after, the mixture is filtered using a vacuum filter holder. After the filter cake is washed adequately with ethanol and acetone, it is dried in an oven at 80 ºC for 6 h. The as-prepared Pd/C catalysts are denoted as Pd/C-t-a, where "t" is the reaction temperature; "a" is the amount of the adding KOH solution in the reaction system. The specific correspondence expression to the catalysts obtained at 200 and 180 ºC are Pd/C-200-3.4, Pd/C-200-4.4, Pd/C-200-5.4, Pd/C-200-6.4, Pd/C-200-7.4, Pd/C-180-3.4, Pd/C-180-4.4, Pd/C-180-5.4, Pd/C-180-6.4 and Pd/C-180-7.4, respectively.

2.2 Characterization of the Pd/C catalysts

JEM 1200EX transmission electron microscope (TEM, JEOL, Japan), Bruker D8 advanced X-ray diffractometer, and Agilent 7500ce ICP-MS (Inductively coupled plasma mass spectrometry) are employed to investigate the surface topography, structure and Pd loading of the Pd/C catalysts.

2.3 Electrochemical studies

The electrooxidation of methanol on the Pd/C catalysts are tested using a CHI 760E electrochemical workstation (Shanghai, China) in the deoxygenated 0.1 M KOH solution with 1 M CH_3OH at 25 ºC. The working electrode is fabricated according to the method described in literature [26-28]. A saturated Ag|AgCl electrode and a graphite electrode (2 cm^2) are used as the reference electrode and counter electrode, respectively.

3. RESULTS AND DISCUSSION

3.1 Catalyst characterization

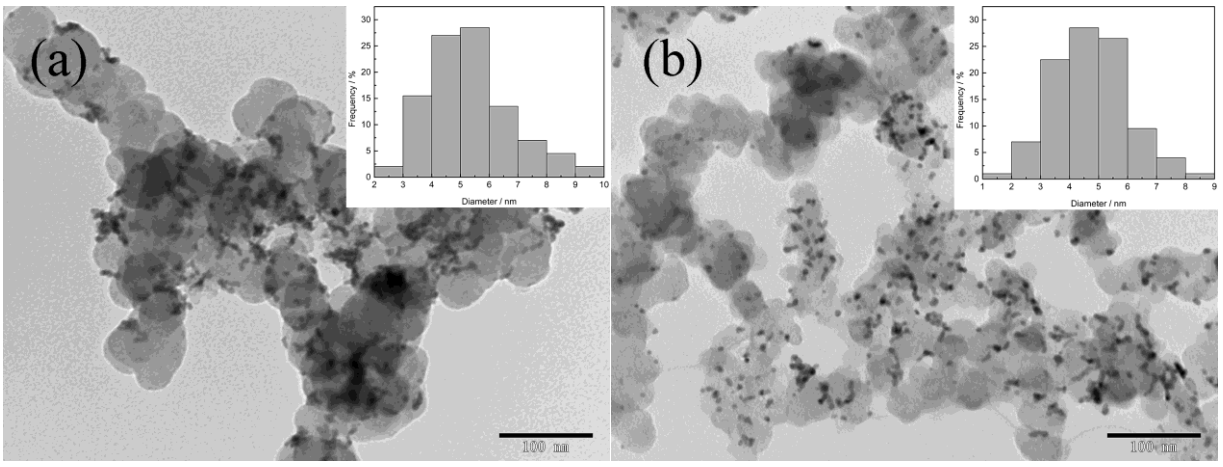

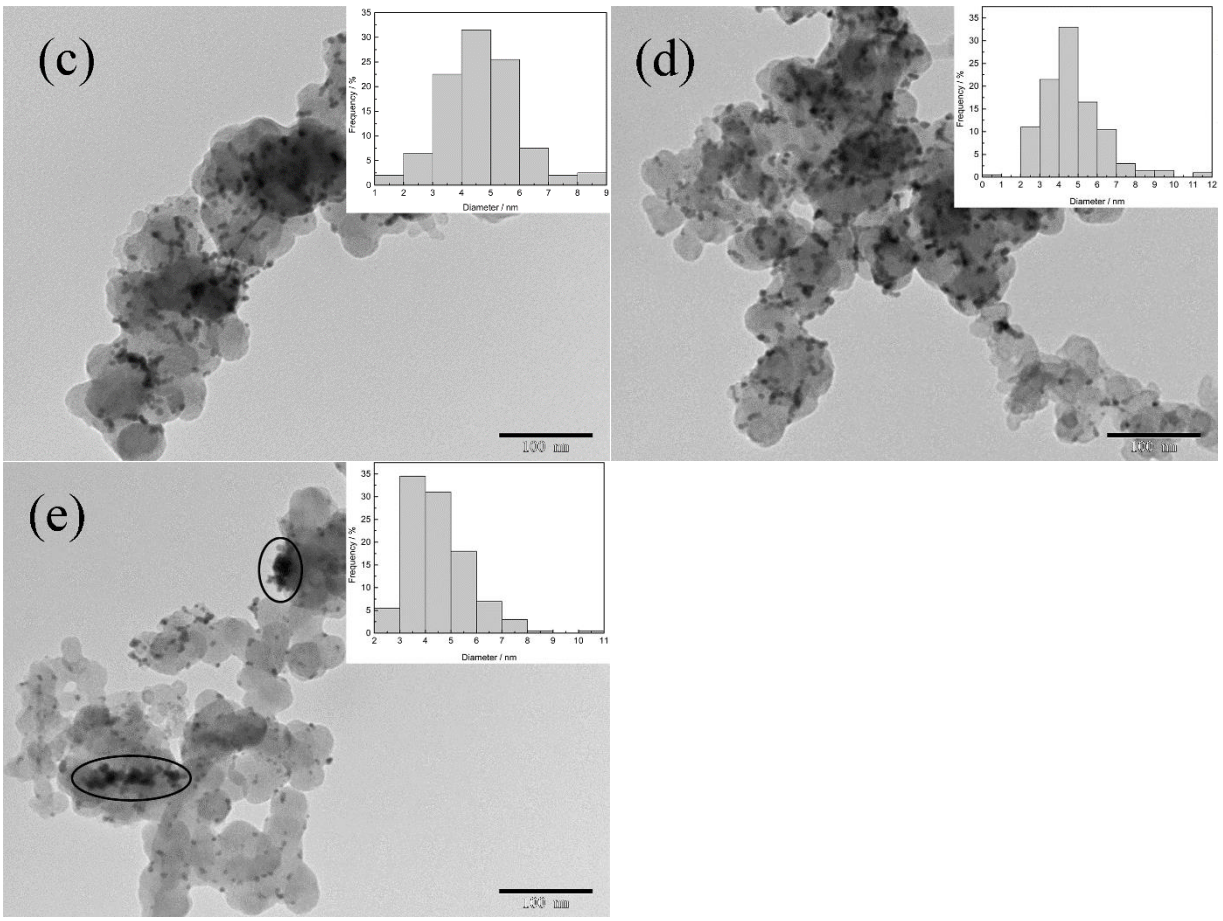

Figure 1. TEM images and corresponding particle diameter histogram of the Pd/C-200-3.4 (a), Pd/C-200-4.4 (b), Pd/C-200-5.4 (c), Pd/C-200-6.4 (d) and Pd/C-200-7.4 (e) catalysts. Scale bar: 100 nm.

Figure 1 is the TEM images of the Pd/C catalysts prepared at 200 ºC under different amount of 1 M KOH solution. It can be seen from the Figure 1 that Pd nanoparticles in each Pd/C catalyst are successfully deposited on the surface of the vulcan XC-72R activated carbon. The distribution of the Pd nanoparticles indicated that, the average diameters of the nanoparticles inthe Pd/C-200-3.4, Pd/C-200-4.4, Pd/C-200-5.4, Pd/C-200-6.4and Pd/C-200-7.4 catalysts are about 5.4, 4.7, 4.7, 4.7 and 4.5 nm, respectively. The mean diameter of Pd nanoparticles in the Pd/C catalyst decreases with the amount of KOH solution. This result is related to the growth mechanism of the Pd nanoparticles, namely the nucleation and growth of the Pd nanoparticles. Since the reducing CH_3CHO species is produced when ethylene glycol is heated in alkaline media [23-25], the reducibility of the reaction systemenhances with the amount of KOH solution. The strong reducibility of the reaction system makes the nucleation rate of the Pd nanoparticles is accelerated, which causes the amount of the Pd nanoparticles increases, resulting in the mean diameter of Pd nanoparticles in the Pd/C catalyst decreases with the amount of KOH solution. It is found from Figures 1a-e that the Pd nanoparticles in the Pd/C-200-3.4, Pd/C-200-4.4, Pd/C-200-5.4, andPd/C-200-6.4 catalysts hardly have any obvious gathering. Figure 1f reveal that, however, the Pd nanoparticles in the Pd/C-200-7.4 catalysts are partially accumulated together, which is indicated by the elliptic area in Figure 1f. This result is related to the high surface activation energy

of the Pd nanoparticles in the Pd/C-200-7.4 catalyst, due to its small size.

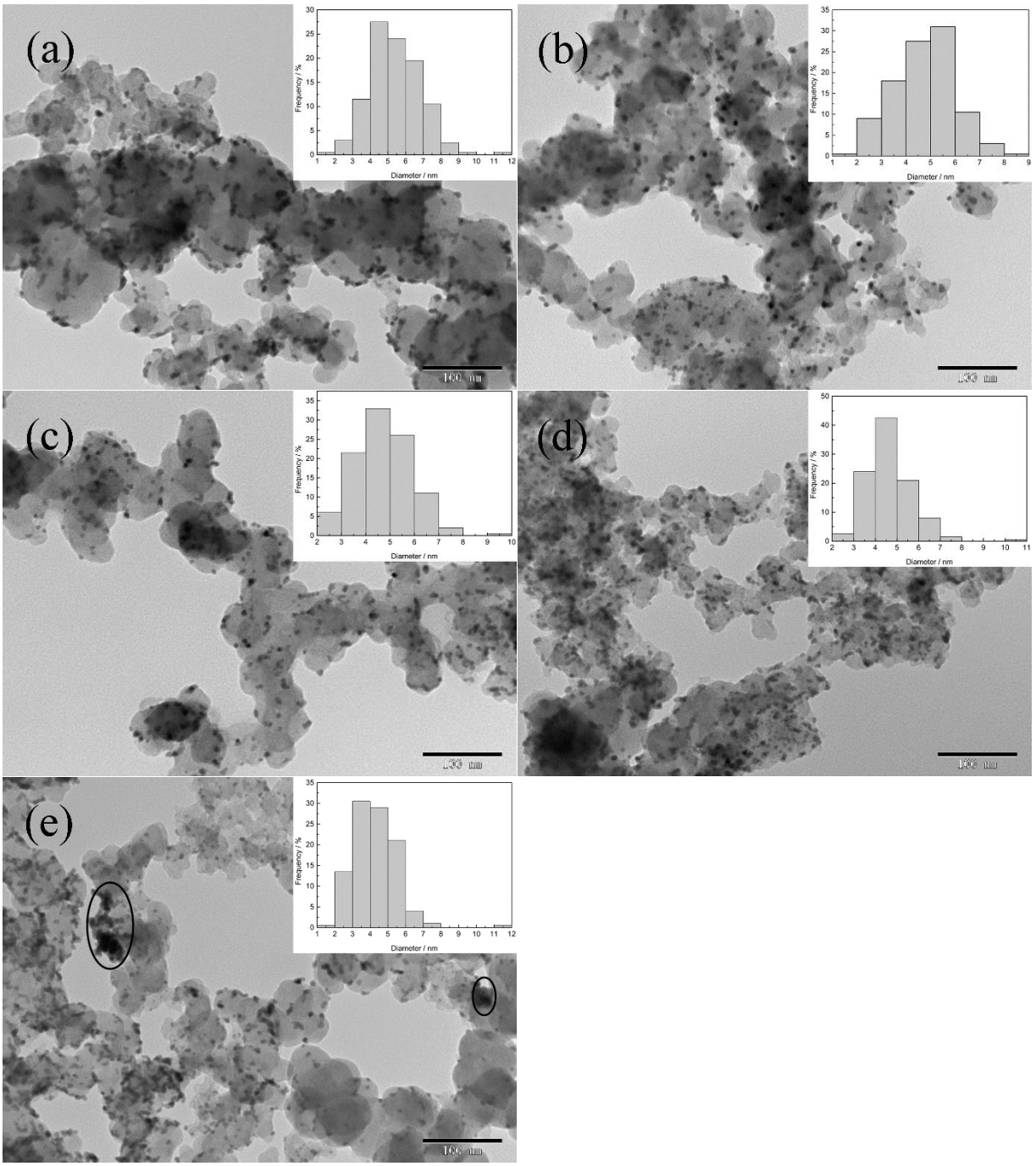

Figure 2. TEM images and corresponding particle diameter histogram of the Pd/C-180-3.4 (a), Pd/C-180-4.4 (b), Pd/C-180-5.4 (c), Pd/C-180-6.4 (d) and Pd/C-180-7.4 (e) catalysts. Scale bar: 100 nm.

For studying the effect of the reaction temperature on the morphology and electrochemical activity of the Pd/C catalyst, the Pd/C catalysts are also synthesized at 180 ºC. Figure 2 reveals the TEM images and the corresponding particle diameter histogram of the Pd/C-180 catalysts. As can be

seen from Figure 2, the average diameters of the nanoparticles inthe Pd/C-180-3.4, Pd/C-180-4.4, Pd/C-180-5.4, Pd/C-180-6.4 and Pd/C-180-7.4 catalysts are about 5.4, 4.7, 4.7, 4.7 and 4.3 nm, respectively. The mean size of the Pd nanoparticles in Pd/C catalyst prepared at 180 ºC decreases with the amount of KOH solution, which is similar to Pd/C catalyst prepared at 200 ºC. With the decrease of the mean size, moreover, the Pd nanoparticles are also partially gotten together, which can be seen from the elliptic region shown in Figure 2e.

It is found from Figure 1 that the morphology of Pd nanoparticles on the Pd/C-200-4.4, Pd/C-200-5.4, Pd/C-200-6.4, Pd/C-200-7.4 and Pd/C-200-8.4 catalysts is spherical; while the Pd nanoparticles on the Pd/C-200-3.4 catalyst present linear profile in nature. This is associated with the reducibility of the reaction system, which enhances with the amount of KOH solution. Therefore, the reducibility of the reaction system for preparing the Pd/C-200-3.4 catalyst is weaken than that of another Pd/C catalyst synthesized at 200 ºC, which causes that the nucleation rate of the Pd nanoparticles in the Pd/C-200-3.4 catalyst is the slowest among the Pd/C catalysts synthesized at 200 ºC. Another reason is that, the growth of the Pd nuclei along a certain direction, due to the adsorption of Cl^- on some specific crystal planes, which likes the adsorption of Br^- [29]. Therefore, the Pd nuclei are grown slowly and along a certain direction to form Pd nanorods with short length. Figure 2 displays that the Pd nanoparticles on the Pd/C-180-3.4 catalyst also present thread-like profile, which is also caused by the weak reducibility of the reaction system, and the orientation growth of the Pd nuclei.

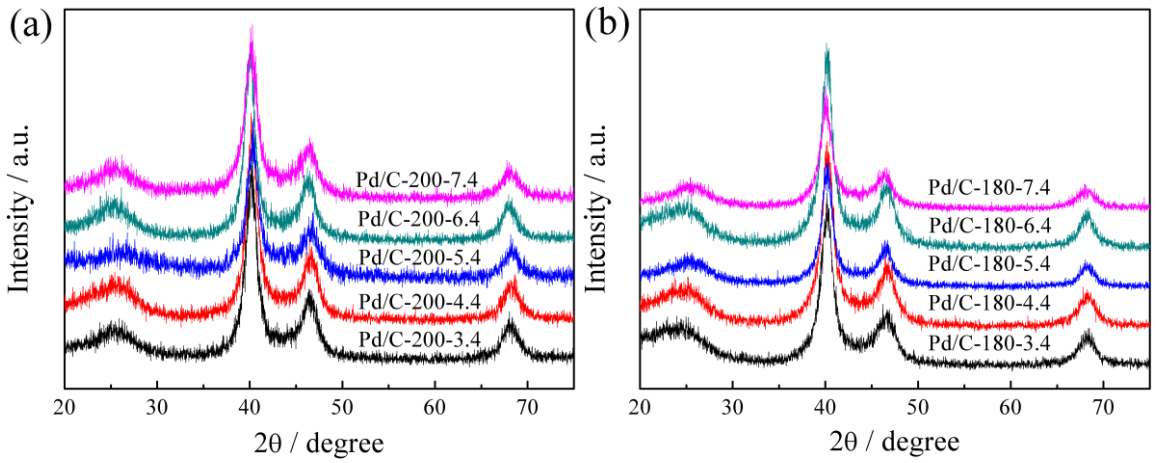

Figure 3. XRD patterns of the Pd/C catalysts prepared at 200 (a) and 180 ºC (b).

Figure 3 shows the XRD patterns of the Pd/C catalysts. The diffraction peak at about 2θ = 25.1° in each XRD pattern corresponds to the (002) plane of graphite (JCPDS, No. 74-2330), which comes from the activated carbon. The diffraction peaks of the (111), (200) and (220) lattice planes of palladium (JCPDS, No. 46-1043) are located at about 2θ = 40.2, 46.8 and 68.2°, respectively, which are characteristic of the face-centered cubic (fcc) structure of Pd [30-32]. All the Pd diffraction peaks exhibit a large width, due to the size effect or nano effect [33]. This phenomenon can be explained using the Scherrer equation [34-36].

Table 1. Metal loading of the catalysts measured by ICP-MS

Catalyst	Actual Pd loading (wt%)	Theoretical Pd loading (wt%)
Pd/C-200-3.4	21.4	20.0
Pd/C-200-4.4	19.6	20.0
Pd/C-200-5.4	212	20.0
Pd/C-200-6.4	20.7	20.0
Pd/C-200-7.4	21.5	20.0
Pd/C-180-3.4	19.1	20.0
Pd/C-180-4.4	19.5	20.0
Pd/C-180-5.4	21.3	20.0
Pd/C-180-6.4	20.9	20.0
Pd/C-180-7.4	18.0	20.0

The testedPd loadings of the Pd/C-200-3.4, Pd/C-200-4.4, Pd/C-200-5.4, Pd/C-200-6.4, Pd/C-200-7.4, Pd/C-180-3.4, Pd/C-180-4.4, Pd/C-180-5.4, Pd/C-180-6.4 and Pd/C-180-7.4 catalysts respectively are 21.4, 19.6,20.7, 21.2, 19.2, 19.1, 19.5, 21.3, 20.9 and 18.0 wt%, which are listed in Table 1. The Pd loadings of all the Pd/C catalysts are around the theoretical loading (20 wt%), showing the high loading efficiency of the Pd nanoparticles on the surface of the activated carbon. The result that the Pd loadings of partial Pd/C catalysts are higher than 20 wt% may be caused by the experimental error. Moreover, the lowest loading efficiency of the Pd is 90 %, which fully proves that the polyol process is a highly efficient synthesis method for reducing Pd^{2+} to Pd.

3.2 Electrochemical studies

The CVs on the Pd/C catalysts prepared at 200 and 180 ℃ tested in 0.1 M KOH and 1 M CH_3OH mixed solution at 25 ℃ are shown in Figures 4a and 4b, respectively. The scan rate is 50 mV s^{-1}. The current densities are normalized by the actual Pd loadings measured by ICP-MS.

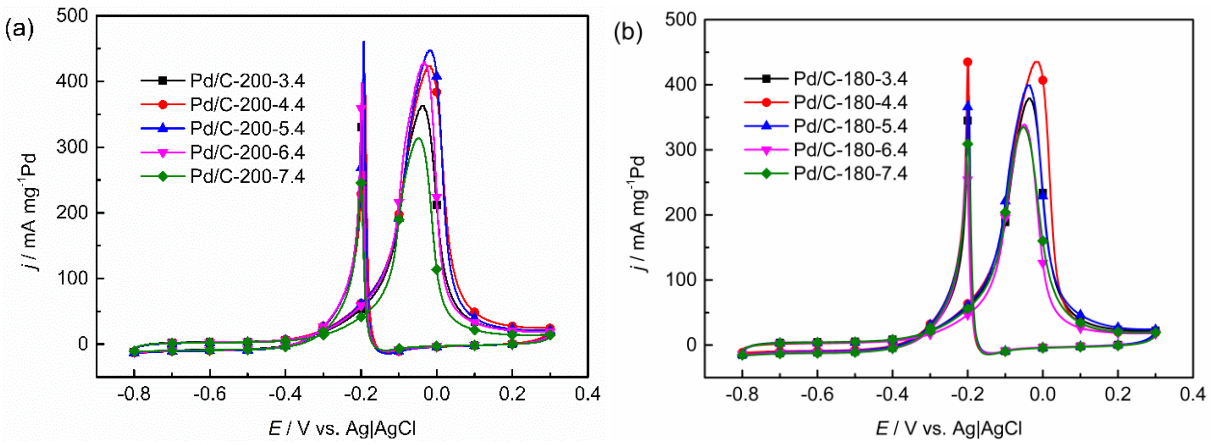

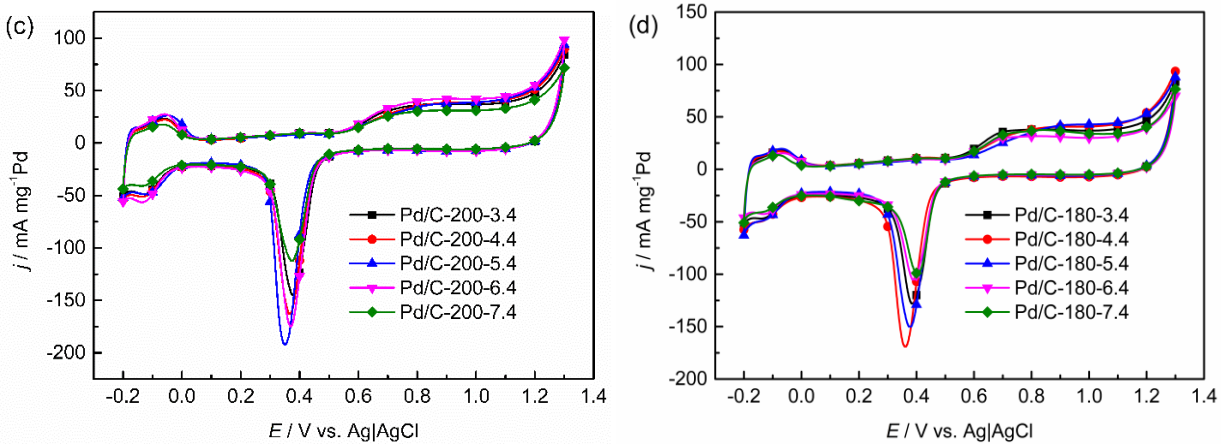

Figure 4. CVs on the Pd/C catalysts prepared at 200 (a) and 180 °C (b) in 0.1 M KOH and 1 M CH_3OH mixed solution at a scan rate of 50 mV s^{-1} at 25 °C. CVs on the Pd/C catalysts prepared at 200 (c) and 180 °C (d) in 0.5 M H_2SO_4 solution at a scan rate of 50 mV s^{-1} at room temperature. The current densities are normalized by the actual Pd loadings.

As is presented in Figure 4, the initial oxidation potential of the methanol on all the Pd/C catalyst is about -0.5 V during the positive-going potential sweep. Furthermore, the peak of the anodic mass-specific current density for the methanol electrooxidation on the Pd/C catalyst appears at about -0.05 V [37-41]. As can be seen from Figure 4a, the peak values of the anodic mass-specific current densities for the methanol electrooxidation on the Pd/C-200-3.4, Pd/C-200-4.4, Pd/C-200-5.4, Pd/C-200-6.4and Pd/C-200-7.4 catalysts are 363.4, 423.4, 447.4, 429.9 and 313.9 mA mg^{-1} Pd, respectively. According to Figure 4b, the peak values of the anodic mass-specific current densities for the methanol electrooxidation on the Pd/C-180-3.4, Pd/C-180-4.4, Pd/C-180-5.4, Pd/C-180-6.4 and Pd/C-180-7.4 catalysts are 379.0, 435.8, 399.4, 339.4 and 334.6 mA mg^{-1} Pd, respectively. It is found that, there is a same trend in the anodic mass-specific current densities for the methanol electrooxidation on the Pd/C catalysts prepared at 200 and 180 °C. It is that the anodic mass-specific current densities increase initially and then decrease with the enhancement in the amount of KOH solution. This phenomenon relates to the distribution and the mean size of the Pd nanoparticles in the Pd/C catalysts. The TEM and XRD results indicate that the mean size of the Pd nanoparticles in the Pd/C-200 and Pd/C-180 catalysts decrease with the increasement in the amount of KOH solution, which makes the activities of Pd/C catalysts enhance with the amount of KOH solution. However, the TEM result shows that the Pd nanoparticles are partially condensed together with the reduction of the mean size, which results in the activities of Pd/C catalysts decrease with the amount of KOH solution. Therefore, the activities of the Pd/C-200-5.4 and Pd/C-180-4.4 catalysts are highest respectively among the Pd/C catalysts prepared at 200 and 180 °C. The reason is the Pd nanoparticles in the Pd/C-200-5.4 and Pd/C-180-4.4 catalysts have small average size and excellent dispersion at the same time. For comparing, the activities of the as-prepared catalyst and the Pd/C catalyts reported in literatures are shown in Table 2 [9,41,42]. The result verifies the great potential of the polyol process in the preparation of Pd/C catalyst with high activity.

Table 2. The activities of Pd/C catalysts in this work and reported in literatures for the methanol oxidations

Catalyst	Electrolytes	Current (mA mg^{-1} Pd)	Ref.
Pd/C	0.1 M KOH + 1 M CH_3OH	About 353.4	[9]
Commercial Pd/C	1 M KOH + 1 M CH_3OH	About 367.9	[41]
Pd/C-DEG	1 M KOH + 1 M CH_3OH	About 420.0	[42]
Pd/C-200-5.4	0.1 M KOH + 1 M CH_3OH	About 447.4	This work
Pd/C-180-4.4	0.1 M KOH + 1 M CH_3OH	About 435.8	This work

To further study the impact of size and structure on the electrochemically active surface area (ECSA) of the Pd/C catalysts, the CVs cures are recorded in 0.5 H_2SO_4. As displayed in Figure 4c and 4d, the current peak appearing at 0.2-0.6V during the negative scanning is attributed to the reduction of PdO to Pd, which can be used to evaluate the electrochemical active surface area (ECSA) of the catalyst [44,45]. According to the equation of ECSA = Q/0.43×[Pd] [44], the ECSA of the Pd/C-200-3.4, Pd/C-200-4.4, Pd/C-200-5.4, Pd/C-200-6.4, Pd/C-200-7.4, Pd/C-180-3.4, Pd/C-180-4.4, Pd/C-180-5.4, Pd/C-180-6.4 and Pd/C-180-7.4 catalysts are about 479.0, 520.8, 604.5, 544.1, 381.3, 409.2, 506.9, 488.3,353.4, 274.4 cm^2 mg^{-1} Pd. The Pd/C-200-5.4 and Pd/C-180-4.4 catalyst exhibit the largest ECSA, respectively. Since the aggregation of particles seriously affects the active surface area of the catalyst, the Pd/C-200-7.4 and Pd/C-180-7.4 catalysts show a relatively small active surface area.

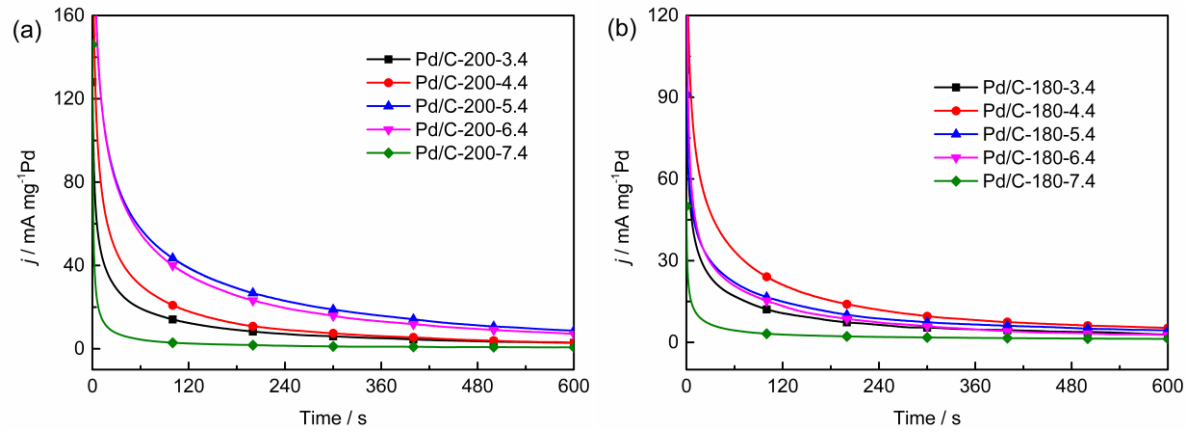

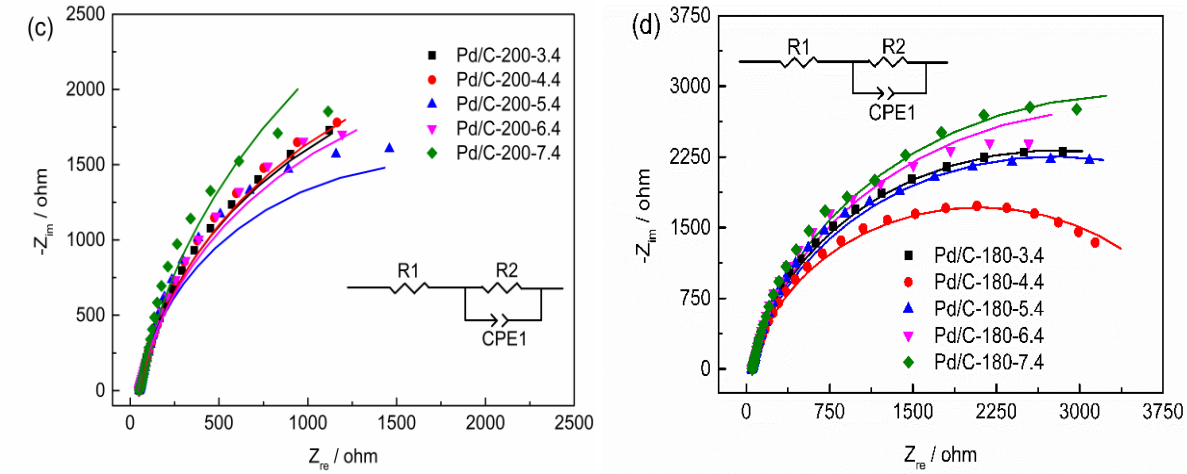

Figure 5. Chronoamperometry curves collected for 600 s at -0.06 V vs. Ag|AgCl on the Pd/C-200 (a) and Pd/C-180 (b) catalysts in the nitrogen saturated 0.1 M KOH + 1 M CH_3OH mixed solution. Nyquist plots of methanol electrooxidation on the Pd/C-200 (c) and Pd/C-180 (d) catalysts in 0.1 M KOH + 1 M CH_3OH mixed solution at the potential of -0.06 V vs. Ag|AgCl.

The stabilities of the as-prepared catalysts are investigated using chronoamperometry in the nitrogen saturated 0.1 M KOH + 1 M CH_3OH mixed solution. The chronoamperograms on the Pd/C catalysts for the MEO are presented in Figure 5, which exhibit that the current densities for the MEO on the Pd/C-200-3.4, Pd/C-200-4.4, Pd/C-200-5.4, Pd/C-200-6.4, Pd/C-200-7.4, Pd/C-180-3.4, Pd/C-180-4.4, Pd/C-180-5.4, Pd/C-180-6.4 and Pd/C-180-7.4 catalysts are about 2.8, 3.0, 8.7, 7.1, 0.7, 2.8, 5.3, 4.4, 2.7 and 1.3 mA mg^{-1} Pd, respectively. In particular, the Pd/C-200-5.4 catalyst exhibits the best stability among these catalysts. These outcomes are owed to the small size and excellent distribution of the Pd nanoparticles in Pd/C-200-5.4 catalyst.

Table 3. The EIS Parameters of the catalysts

Catalyst	0.1 M KOH + 1 M CH3OH			
	R1 (ohm)	R2 (ohm)	CPE1-T (μF)	CPE1-P(μF)
Pd/C-200-3.4	53.9	5943	0.00015166	0.89671
Pd/C-200-4.4	48	5767	0.00015016	0.89163
Pd/C-200-5.4	52.23	4122	0.00017239	0.9078
Pd/C-200-6.4	51.74	5157	0.00013111	0.91007
Pd/C-200-7.4	51.59	8297	0.00019124	0.90132
Pd/C-180-3.4	52.57	5615	0.00016256	0.88244
Pd/C-180-4.4	56.45	4132	0.0001308	0.8904
Pd/C-180-5.4	48.84	5543	0.00014838	0.89774
Pd/C-180-6.4	52.11	6601	0.00017104	0.88547
Pd/C-180-7.4	53.52	7072	0.00014336	0.89614

The electrochemical impedance spectroscopy (EIS) spectra of the Pd/C catalysts for the MEO are analyzed and explained by equivalent circuit inserted in Figure.5c and 5d [46]. R1 and R2 reflect

the resistance of the electrolyte and the electrode, as well as the charge transfer resistance of the electrochemical reactions; CPE1 corresponds the related electric double layer capacitance of the electrochemical reactions. The corresponding parameters are presented in Table 3. The values of the R2 corresponds to the radius of the arc in the Figure 5, which increases in the order of Pd/C-200-5.4, Pd/C-200-6.4, Pd/C-200-4.4, Pd/C-200-3.4,Pd/C-200-7.4 and Pd/C-180-4.4, Pd/C-180-5.4, Pd/C-180-3.4, Pd/C-180-6.4, Pd/C-180-7.4 catalysts. This result shows that the charge transfer resistances of the MEO on the Pd/C-200-5.4 and Pd/C-180-4.4 catalysts are smaller than others, which is also related to the small size and excellent distribution of the Pd nanoparticles in these catalysts.

4. CONCLUSIONS

A series of Pd/C catalysts is successfully synthesized by the polyol process at 200 and 180 ℃. The characterization of the Pd/C catalysts reveals that the Pd nanoparticles in the Pd/C catalysts are successfully deposited on the surface of the carbon support, as well as their mean size decrease with the enhancement in the amount of KOH solution. However, the Pd nanoparticles in the Pd/C catalysts are partially accumulated together, due to the high surface activation energy of the Pd nanoparticles with small size. The methanol electrooxidation test results reveal the activities of the Pd/C-200-5.4 and Pd/C-180-4.4 catalysts are highest respectively among the Pd/C catalysts prepared at 200 and 180 ℃, since their Pd nanoparticles have small average size and excellent dispersion at the same time. Moreover, the Pd/C catalysts with good activity can be prepared at 200 and 180 ℃, showing that the polyol process is suitable for the preparation of Pd/C catalyst with high activity.

ACKNOWLEDGEMENT
We greatly appreciate the Major Science and Technology (20181102019) and Natural Science Foundation (2014011017-2) projects of Shanxito fund this work.

References

1. H.S. Liu, C.J. Song, L. Zhang, J.J. Zhang, H.J. Wang, D.P. Wilkinson, *J. Power Sources,* 155 (2006) 95.
2. A. Kuver, S. Wasmus, *J. Electroanal. Chem.*, 461 (1999) 14.
3. A.S. Aricò, S. Srinivasan, V. Antonucci, *Fuel Cells,* 1 (2015) 133.
4. A. Mehmood, M.A. Scibioh, J. Prabhuram, M. An, H.Y. Ha, *J. Power Sources,* 297 (2015) 224.
5. K. Matsuoka, Y. Iriyama, T. Abe, M. Matsuoka, Z. Ogumi, *J. Power Sources,* 150 (2005) 27.
6. E.A. Monyoncho, S. Ntais, F. Soares, T.K. Woo, E.A. Baranova, *J. Power Sources,* 287 (2015) 139.
7. M. Farsadrooh, J. Torrero, L. Pascual, M.A. Peña, M. Retuerto, S. Rojas, *Appl. Catal., B,* 237 (2018) 866.
8. M. ZareieYazdan-Abad, M. Noroozifar, N. Alfi, A.R. Modarresi-Alam, H. Saravani, *Int. J. Hydrogen Energy,* 43 (2018) 12103.
9. Y. Yamauchi, A. Tonegawa, M. Komatsu, H. Wang, L. Wang, Y. Nemoto, N. Suzuki, K. Kuroda, *J.*

Am. Chem. Soc., 134 (2012) 5100.
10. W. Liang, Y. Yamauchi, *Chem. Mater.*, 23 (2011) 2457.
11. B.M. Hunter, W. Hieringer, J.R. Winkler, H.B. Gray, A.M. Müller, *Energy Environ. Sci.*, 9 (2016) 1734.
12. X.Y. Jin, J. Lim, N.S. Lee, S.J. Hwang, *Electrochim. Acta*, 235 (2017) 720.
13. S.S. Li, J.J. Lv, Y.Y. Hu, J.N. Zheng, J.R. Chen, A.J. Wang, J.J. Feng, *J. Power Sources,* 247 (2014) 213.
14. J.C. Bertolini, *Catal. Today,* 138 (2008) 84.
15. S.E. Habas, L. Hyunjoo, R. Velimir, G.A. Somorjai, Y. Peidong, *Nat. Mater.*, 6 (2007) 692.
16. M.M. Liu, Y.Z. Lu, C. Wei, *Adv. Funct. Mater.*, 23 (2013) 1289.
17. M. Dehvari, H. Saravani, N. Akbarzadeh, M.Z. Yazdan-Abad, *Int. J. Hydrog. Energy,* 44 (2019) 6544.
18. R. Muszynski, B. Seger, P.V. Kamat, *J. Phys. Chem. C,* 112 (2008) 5263.
19. M.K. Carpenter, T.E. Moylan, K. Ratandeep Singh, M.H. Atwan, M.M. Tessema, *J. Am. Chem. Soc.*, 134 (2012) 8535.
20. J.B. Wu, J.L. Zhang, Z.M. Peng, S.C. Yang, F.T. Wagner, H. Yang, *J. Am. Chem. Soc.*, 132 (2010) 4984.
21. X.M. Chen, G.H. Wu, J.M. Chen, X. Chen, Z.X. Xie, X.R. Wang, *J. Am. Chem. Soc.*, 133 (2011) 3693.
22. Y.J. Yang, *Int. J. Electrochem. Sci.*, 14 (2019) 1270.
23. S.H. Yan, S.C. Zhang, W.K. Zhang, L. Jin, L.Z. Gao, Y.Q. Yang, Y.H. Gao, *J. Phys. Chem. C,* 118 (2014) 29845.
24. Z.L. Liu, L. J.Y. Lee,W.X. Chen, M. Han, L.M. Gan, *Langmuir,* 20 (2004) 181.
25. X. Li, W.X. Chen, J. Zhao, W. Xing, Z.D. Xu, *Carbon,* 43 (2005) 2168.
26. S.H. Yan, S.C. Zhang, L. Ye, G.R. Liu, *J. Phys. Chem. C,* 115 (2011) 6986.
27. S.H. Yan, L.Z. Gao, S.C. Zhang, L.L. Gao, W.K. Zhang, Y.Z. Li, *Int. J. Hydrog. Energy,* 38 (2013) 12838.
28. S.H. Yan, L.Z. Gao, S.C. Zhang, W.K. Zhang, Y.Z. Li, L.L. Gao, *Electrochim. Acta,* 94 (2013) 159.
29. W.X. Niu, G.B. Xu, *Nano Today*, 6 (2011) 265.
30. C. Shang, W. Hong, Y. Guo, J. Wang, E. Wang, *Chem-Eur J*, 23 (2017) 5799.
31. H. Wei, P.Y. Bi, C.S. Shang, W. Jin, E.K. Wang, *J. Mater. Chem. A*, 4 (2016) 4485.
32. Y.J. Huang, X.C. Zhou, J.H. Liao, C.P. Liu, T.H. Lu, W. Xing, *Electrochem. Commun.*, 10 (2008) 1155.
33. H.Tsunoyama, H. Sakurai, N. Ichikuni, Y. Negishi, T. Tsukuda, *Langmuir,* 20 (2004) 11293.
34. Z.L. Liu, B. Guo, L. Hong, T.H. Lim, *Electrochem. Commun.*, 8 (2006) 83.
35. Y.R. Wang, Q.L. He, K.Q. Ding, H.G. Wei, J. Guo, Q. Wang, R. O'Connor, X.H. Huang, Z.P. Luo, T.D. Shen, S.Y. Wei, Z.H. Guo, *J. Electrochem. Soc.*, 162 (2015) F755.
36. Z.P. Sun, X.G. Zhang, R.L Liu, Y.Y. Liang, H.L. Li, *J. Power Sources*, 185 (2008) 801.
37. Y.T. Zhang, H.H. Shu, C. Gang, J. Kai, M. Oyama, L. Xiong, Y.B. He, *Electrochim. Acta,* 109 (2013) 570.
38. Z.S. Li, L.T. Ye, Y.L. Wang, S.H. Xu, F.L. Lei, S. Lin, *RSC Adv.*, 6 (2016) 79533.
39. J.S. Moon, Y.W. Lee, S.B. Han, K.W. Park, *Int. J. Hydrog. Energy,* 39 (2014) 7798.
40. Z.P. Sun, X.G. Zhang, Y.Y. Liang, H.L. Li, *Electrochem. Commun.*, 11 (2009) 557.
41. Z.P. Sun, X.G. Zhang, R.L. Liu, Y.Y. Liang, H.L. Li, *J. Power Source*s, 185 (2008) 801.
42. H.Q. Ye, Y.M. Li, J.H. Chen, J.L. Sheng, X.Z. Fu, R. Sun, C.P. Wong, *J Mater Sci,* 53 (2018) 15871.
43. Y.N. Zhai, S. He, X. Xiao, Z.Q. Wu, S.N. Li, *Fuel Cells*, 16 (2016) 771.
44. Y. Feng, D. Bin, B. Yan, Y. Du, T. Majima, W. Zhou, *J. Colloid Interface Sci.*, 493 (2017) 190.
45. J.L. Tan, A.M. De Jesus, S.L. Chua,J. Sanetuntikul, S. Shanmugam, B.J.V. Tongol, H. Kim, *Appl Catal A-Gen*, 531 (2017) 29.

46. Z. He, F. Mansfeld, *Energy Environ. Sci.*, 2 (2009) 215.